Jordan Journal of Civil Engineering, Volume **12**, No. **2**, **2018**

Nonlinear Finite Element Modeling of GFRP-Strengthened Slender Rectangular RC Columns with Confinement Deficiency in Plastic Hinge Zone

***V. Zanjani Zadeh*[1)]* *and S. Eshghi*[2)]**

[1)] Former Research Associate, 3100, Post Oak Blvd., Houston, Texas, USA.
* Corresponding Author. E-Mail: vzanjan@ncsu.edu
[2)] Associate Professor, International Institute of Earthquake Engineering and Seismology (IIEES), Tehran, Iran.
E-Mail: s.eshghi@iiees.ac.ir

ABSTRACT

This paper presents a study on the behavior of slender Reinforced Concrete (RC) columns, with confinement deficiency in plastic hinge zone, strengthened with Glass Fiber-Reinforced Polymer (GFRP) sheets using Finite Element Analysis (FEA). For the purpose of this research, a total of twelve half-scale rectangular RC columns were modeled using ANSYS and subjected to displacement-controlled monotonic lateral load combined with a constant axial load. Ten out of the twelve columns had insufficient transverse reinforcements in the plastic hinge zone to represent the columns that were built before 1971. Five columns were retrofitted up to recommended length from bottom of the column with GFRP wraps. The goal of these analyses was to investigate failure mechanism and to obtain the lateral load-carrying capacity of the columns, as well as to compare them with existing experimental hysteresis loop envelope available from cyclic loading tests. The developed FEA predictions were shown to be in close agreement with the experimental results and observations. The results showed that the FRP jacket in plastic hinge zone can greatly enhance shear and flexural strengths, as well as ductility of the slender RC columns under imposed loading and that it delays the softening of the columns.

KEYWORDS: Slender reinforced concrete columns, Glass fiber-reinforced polymer, Finite element analysis, Plastic hinge zone, Lateral load-carrying capacity.

INTRODUCTION

Experiences from past strong earthquakes, such as the Kobe (Japan-1995), Izmit (Turkey-1999), Chi-chi (Taiwan-1999), Gujarat (India-2001), Boumerdes (Algeria-2003), Bam (Iran-2003), Offshore Bio-Bio (Chile -2010) and Haiti (Haiti-2010), have revealed the vulnerability of RC columns to strong ground shaking. Columns are important structural members and failure of columns can lead to total or partial collapse of buildings (Moehle et al., 2006). Incorrect detailing, flaws in design and/or construction practices can make columns extremely vulnerable to earthquakes, which can lead to brittle failure without any ductility. For example, insufficient confinement in plastic hinge zone, which provides little to no ductility, can cause premature failure of materials, such as early crushing of confined concrete, as a result of concrete low strength, sliding of longitudinal reinforcements prior to yielding, opening of the ties and eventually shear or flexural failure in columns (Lynn et al., 1996). Older RC columns in

Received on 7/5/2015.
Accepted for Publication on 4/7/2015.

regions of high seismicity, which were designed prior to advent of modern design codes ACI (Pre-1971), have the same detailing deficiency and will suffer the same failures (Melek and Wallace, 2004; Eshghi and Zanjanizadeh, 2007, 2008). Rehabilitation of these columns has been a matter of growing concern in the past two decades. Studies carried out in the past have shown that compressive strength of concrete core, ultimate compressive strain of concrete and column ductility can be significantly increased by providing suitable ways of external confinement (Priestley et al., 1994; Masukawa et al., 1997; Xiao et al., 1999; Basisu et al., 2012). As evidenced, the retrofitted columns survived the 1994 Northridge earthquake with no or minor damage (Loud, 1995). However, available literature on seismic behavior and strengthening of slender rectangular RC columns, e.g. (Tamuzs et al., 2007; Jiang and Teng, 2013), is still limited. Available previous research mainly focuses on retrofitting columns under axial or uniaxial loading and on short columns (Eshghi and Zanjanizadeh, 2007, 2008).

The use of FRP for repair and retrofit of existing structures has become increasingly popular worldwide during the past two decades and replaced in many cases classical methods due to its high strength-to-weight and stiffness-to-weight ratios, corrosion resistance, easy and rapid installation, minimal change in the column geometry, lightweight and potentially high durability (ACI, 1996; Teng et al., 2002; Einde et al., 2003; Obaidat, 2013). Also, strengthening of columns with FRP has demonstrated to be a promising technique to remedy the vulnerability of RC columns with structural deficiencies (Eshghi and Zanjanizadeh, 2007, 2008; Al-Dwaik and Armouti, 2013). Consequently, many studies have been devoted to the behavior and modeling of FRP-confined concrete for circular, e.g. (Samaan et al., 1998; Yu et al., 2010; Pellegrino and Modena, 2010) and rectangular, e.g. (Chaallal et al., 2003; Sheikh and Li, 2007; Wu et al., 2007) cross-sections.

Several researches showed that the Finite Element (FE) numerical simulation is an efficient method for studying confined RC columns with FRP sheets (Rochette and Labossiere, 1996; Mirmiran et al., 2000; Parvin et al., 2001; Feng et al., 2002). In most of these studies, RC columns were fully wrapped with FRP sheets and analyzed under uniaxial loading. However, assuming columns as purely concentric members contradicts with reality, since eccentricities commonly exist *in situ* and should be taken into account in FE modeling.

Due to complexity of the composite behavior of FRP and RC members, presenting an appropriate numerical model for the nonlinear analysis of FRP-retrofitted poorly confined slender columns is a matter of great importance. In the present study, FE models have been developed using ANSYS, in order to understand the inelastic behavior of confined RC columns wrapped with GFRP sheets, as well as to predict the behavior of such strengthened columns in a better way. Only plastic hinge zone was wrapped up to the recommended length from bottom of the columns. From twelve columns, ten were designed according to ACI (Pre-1971) and two according to ACI (318-02) provision. The columns were analyzed under different axial loads and a monotonic lateral displacement. The FEA results were validated using the experimental study reported by the authors elsewhere (Eshghi and Zanjanizadeh, 2008). The results obtained from FEA were consistent with experimental data. It was shown that applying GFRP at plastic hinge zone of slender RC columns can improve their ductility, as well as their shear and flexural strengths.

Column Failures in Past Earthquakes

Past earthquakes showed that failure imposed on columns due to seismic loads can be categorized as follows (Penelis and Kappos, 1997):

1. Failure due to cyclic bending moment and low shear force under large axial force, that usually occurs in slender columns. The α parameter for these columns is defined as:

$$a = \frac{M}{Vh} = \frac{L}{2h} \geq 3.5 \quad (1)$$

where M, V, h and L are bending moment, cyclic

shear force, column smallest cross-section dimension and column height, respectively. Investigated columns in this research belong to this category.

2. Failure due to cyclic shear and low bending moment with high axial force, that occurs in fat columns. The α parameter for this type of column is defined as:

$$a = \frac{M}{Vh} = \frac{L}{2h} < 3.5 \quad (2)$$

3. Failure in splice area of the columns, especially near the bottom of the columns.

Failure in the splice area occurs due to short splice length and/or splicing a large percentage of longitudinal reinforcements in a section, which causes brittleness of that section. Until 1971, the splice length was generally designed for only compressive force; therefore, the buildings constructed in accordance with ACI (Pre-1971) have the problem of short splice length. Also, only light transverse reinforcement is provided over the lap-splice length. Due to poor construction practice, the condition in some developing countries is even worse. Column damage associated with poor performance of splices and confinement has been consistently observed in recent earthquakes. Failures of two columns due to short splice length and large distance of transverse reinforcements are displayed in Fig. 1 and Fig. 2, respectively. Due to the significant contribution of column failures to the collapse of buildings during earthquakes, it is necessary to develop economical methods to upgrade the column capacity, in order to prevent a brittle failure and, instead, shift the failure towards a beam flexural hinging mechanism, which is a more ductile type of behavior (Melek and Wallace, 2004; Eshghi and Zanjanizadeh, 2007).

Figure (1): Failure due to insufficient splice length at the top and bottom of the RC column in Bingöl (Turkey) earthquake, 2003 (NISEE)

Figure (2): Severe damage in the RC column due to widely spaced transverse reinforcements in Columbia earthquake, 1999 (NISEE)

Confinement Effect on Rectangular Cross-Sections

It is well established that transverse reinforcements increase concrete ductility, as well as axial and shear strengths by increasing ultimate strain (Mander et al., 1988). Fig.3 shows stress distribution due to transverse bars in rectangular section under concentric loading. Numbers of confinement models have been introduced for rectangular cross-sections, e.g. (Mander et al., 1988; Chung et al., 2002).

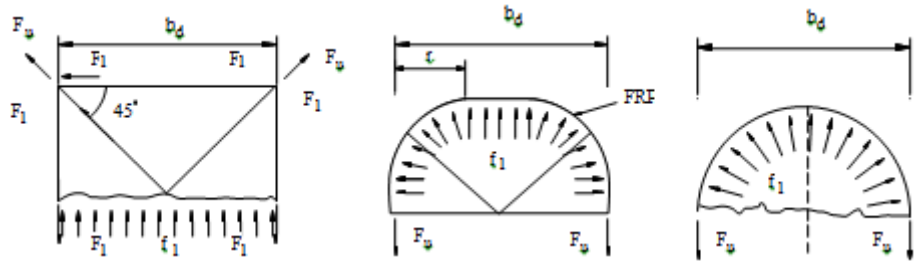

Figure (3): Stress distribution due to transverse bars in rectangular cross-section under concentric loading (Penelis and Kappos, 1997)

Stress distribution of FRP confinement in rectangular and circular cross-sections is shown in Fig. 4. FRP-confined cross-sections can increase the ultimate strain much more than transverse reinforcements (Silva, 2011). Also, the confinement with composite fibers for rectangular cross-sections is less efficient compared to circular cross-sections due to singularity and stress concentration introduced at the corners, as well as the reduced confinement on the flat sides (Campione et al., 2001). Sharp corners in rectangular cross-sections can cause most of the failures which occur at the corners of the cross-section (Fig.4) due to rupture of FRP composites (Silva, 2011).

Numerical Analysis

Column Geometries and Reinforcement Details

Twelve half-scale cantilever RC column models, numbered from SP-C1 to SP-C12, were designed. The columns were modeled with the same configuration and reinforcement details similar to those in experimental studies conducted by other authors in order to verify the results. All the columns had a square cross-section of 150×150 mm and 800 mm height. They were reinforced with 8Φ8 longitudinal bars; however, the transverse reinforcing details of the specimens were different. The details of the specimens are summarized in Table 1. Group I (SP-C1 to SP-C10) was designed according to ACI (Pre-1971) provision, reinforced by 4-mm ties spaced at 150 mm throughout the column. Five columns (SP-C6 to SP-C10) were retrofitted with four layers of bidirectional GFRP sheets up to 240 mm length from bottom of the columns and five other columns were analyzed without rehabilitation measures to serve as benchmarks. The thickness of each FRP layer was approximately 0.2 mm. Characteristics of GFRP sheets are shown in Table 2. Group II (SP-C11 and SP-C12) was designed in accordance with ACI (318-02), enclosed by 4 mm ties spaced at 60 mm at plastic hinge zone and 4 mm ties spaced at 150mm in the rest of the column length, respectively.

All the specimens were studied by displacement-controlled pushover analysis with the axial load held constant for the duration of the analysis. The axial load on the specimens was varied from minimum to maximum values of 0.05 and $0.25A_g \times f'_c$. A_g is the cross-section area and f'_c is the concrete compressive strength.

Table 1. Details of specimens

Specimen	P/ (f'c ×Ag)	Axial Load (kN)	Trans. Reinf.	Retrofitted
SP-C1	0.05	21.2	Φ4@150	No
SP-C2	0.1	42.4	Φ4@150	No
SP-C3	0.15	63.6	Φ4@150	No
SP-C4	0.2	84.8	Φ4@150	No
SP-C5	0.25	106	Φ4@150	No
SP-C6	0.05	21.2	Φ4@150	Yes
SP-C7	0.1	42.4	Φ4@150	Yes
SP-C8	0.15	63.6	Φ4@150	Yes
SP-C9	0.2	84.8	Φ4@150	Yes
SP-C10	0.25	106	Φ4@150	Yes
SP-C11	0.05	21.2	Φ4@60 (240-mm) and Φ4@150	No
SP-C12	0.15	63.6	Φ4@60 (240-mm) and Φ4@150	No

Table 2. Characteristics of the glass-fiber polymers (Eshghi and Zanjanizadeh, 2007)

Ultimate Strain (mm/mm)	Density (N/m^3)	Tensile Strength (MPa)	Elastic Modulus (MPa)	Thermal Expansion Coefficient (1/C°)
0.048	25.5	1750	$7x10^4$	$4.7x10^{-6}$

Stirrup and FRP Confinement Models

The confinement model for concrete used in this analysis is based on a model suggested by Park et al. (1982). This model is a modified version of the Kent and Park (1971) stress and strain curve that takes the effect of cyclic loading in the model into account. As shown in Fig. 4, they assumed that the compressive stress-strain diagram of confined concrete could be divided into three distinct parts: ascending, descending and levelling off. They proposed that the ascending portion was not affected by the confinement and could be described by the second degree parabola. Also, they assumed that the descending part was linear and the final portion of the curve was assumed to be level at 20% of the maximum stress.

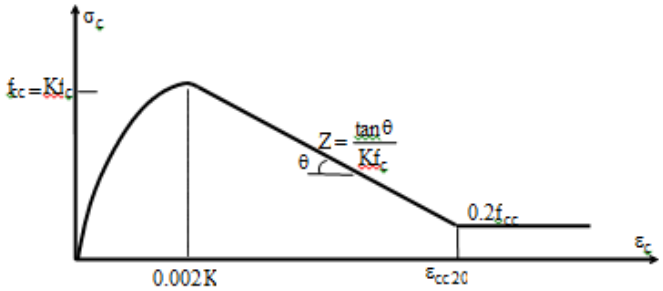

Figure (4): Stress-strain curve of confinement model for stirrup (Park et al., 1988)

This model considers strength and ultimate longitudinal strain enhancement in the zone confined by stirrup and concrete outside stirrup. In this confinement model, the confined concrete stress and strain are computed:

$$K = 1 + \frac{\rho_w f_{yw}}{f_c} \quad (3)$$

$$\varepsilon_{cc50} = \frac{3 + 0.29 f_c}{145 f_c - 1000} + 0.75 \rho_w \left(\frac{b_c}{s} \right)^{\frac{1}{2}} \quad (4)$$

$$z = \frac{0.5}{\varepsilon_{cc50} - \varepsilon_{cc1}} \quad (5)$$

$$f_{cc} = K f_c \quad (6)$$

where K, $\varepsilon_{cc}50$ and $\varepsilon_{cc}1$ are the confinement coefficient, strain corresponding to 50% and maximum compressive strength, respectively.ρ_w, s and f_{yw} are transverse reinforcement percentage, space and yield stress, respectively. f_c and f_{cc} are unconfined and confined compressive strength of concrete, respectively. b_c is the dimension of the confined cross-section. Unconfined compressive strength of concrete was taken from experimental results, then parameters for the confined model were calculated. Finally, the stress-strain curve was inserted into the FE software.

FRP jacket will confine the cover of the column and add additional confinement effect to the zone inside the stirrups. Both of these confinement effects are passive and do not function till columns laterally expand under axial or moment loading. Several studies (Samaan et al., 1998; Kawashima et al., 2001; Pulido et al., 2004) have reported on the stress-strain curve of FRP-wrapped concrete. For the FE model in this study, the FRP confinement model from Pulido et al. (2004) was used. This model is simple to implement, considers most of the characteristics of FRP fibers and is validated by pushover analysis which is the same type of analysis that was carried out in this study. In this model, confinement pressure can be obtained by:

$$f_r = K_e \left(\left(\frac{E_j \varepsilon_j t_j}{d} \right) + \left(\frac{E_j \varepsilon_j t_j}{b} \right) \right) \quad (7)$$

where E_j = elastic modulus of the jacket, ε_j = strain of the jacket in the direction of the fibers, t_j = thickness of the jacket, K_e = shape factor, taken as 0.75 for rectangular cross-sections and d and b = depth and width of the cross-section. Finally, peak confined stress is computed by the following formula:

$$f_{cu} = f_c + 98 f_r^{0.7} \quad (8)$$

Also, ultimate strain of concrete is obtained from the following relationship:

$$\varepsilon_{cu} = \frac{\varepsilon_{cf}}{0.09 - 0.23 Ln\left(\frac{f_r}{f_c} \right)} \quad (9)$$

where ε_{cf} = ultimate FRP jacket strain, taken as 50% of the measured ultimate tensile strain of the FRP. f_c = unconfined concrete strength and f_r = confinement pressure of the jacket. Both are in MPa.

Failure Criteria for Steel, Concrete and FRP

All the mechanical properties of steel, concrete and GFRP were taken from experimental studies. The yield stress and strain of the longitudinal bars were 420 MPa and 0.0017 and those of the stirrups were 300 MPa and 0.0015, respectively. The cylindrical compressive strength, the modulus of elasticity and the Poisson's ratio of concrete were 18.9 MPa, 22000 MPa and 0.2, respectively. Bilinear kinematic hardening model was used in order to model plastic behavior of steel bars. This model needs only yield stress and hardening modulus of steel.

The behavior of confined concrete under loading can be divided into three phases: a) elastic deformation, b) crack formation and propagation and c) plastic

deformation. Therefore, it can be assumed that concrete acts as an Elastic-Perfectly Plastic (EPP) material after reaching its ultimate capacity (Mirmiran et al., 2000). There are many constitutive models for confined concrete as a pressure- and constraint- sensitive material (Mirmiran et al., 2000; Chen and Mau, 1989; Nanni and Bradford, 1995; Fardis and Khalili, 1981; Ahmad et al., 1991; Rochette and Labossiere, 1996; Karabinis and Rousakis, 2002; Issa and Alrousan, 2009). It has been demonstrated by Karabinis and Rousakis (2002) that the nonlinear behavior of concrete structural members can be accurately estimated by Drucker-Prager type plasticity model, which is also adopted in the current study. In this plasticity model, the parameters related to friction angle and cohesion govern the yielding and hardening criteria, while the parameter related to plastic dilation determines the flow rule.

Drucker-Prager criterion is a general form of Von-Mises criterion. According to Chen (1982), the influence of hydrostatic stress component of failure is defined by the additional term in Von-Mises expression. The criterion has the following form:

$$f(I_1,J_2)=\alpha I_1+\sqrt{J_2}-k=0 \tag{10}$$

where $I_1=\sigma_1+\sigma_2+\sigma_3$ and

$$J_2=\left(|\sigma_1-\sigma_2|^2+|\sigma_2-\sigma_3|^2+|\sigma_1-\sigma_3|^2\right)/6$$

are first invariant and second invariant of the stress deviatoric tensor. α is the frictional parameter that expresses the pressure sensitivity of the material and k is the strain hardening function. Rochette and Labossiere (1996) determined α and k for axially loaded FRP-confined columns as follows:

$$\alpha=\frac{5}{f_c} \quad , \quad \frac{k}{f_c}=\frac{1}{\sqrt{3}}-\alpha \tag{11}$$

where f_c is the compressive strength of concrete in MPa. The Drucker–Prager failure criterion can be made to agree with the outer limits of the Mohr–Coulomb hexagon (Chen, 1982). If the two surfaces are made to coincide along the compression meridian, the failure envelope can be modeled as a straight line in terms of the cohesion value of concrete C and the angle of internal friction of concrete φ, as follows:

$$|\tau|=C-\sigma\tan\alpha \tag{12}$$

where τ and σ are the shear and normal stresses, respectively. Using the values of α and λ from Eq. (11), the values of φ and C are obtained as follows:

$$\varphi=Sin^{-1}\left(\frac{15\sqrt{3}}{5\sqrt{3}+2f_c}\right) \tag{13}$$

$$C=\left(f_c-5\sqrt{3}\right)\left(\frac{3-Sin\varphi}{6Cos\varphi}\right) \tag{14}$$

where f_c is the unconfined compressive strength of concrete and C, σ, τ and f_c are in MPa.

Also, the William-Warnke model (William and Warnke, 1975) was used as the failure criterion for concrete. The model assumes that concrete behaves elastically as long as the stress state lies within an initial yield surface. When loading progresses beyond the initial yield surface, plastic flow occurs and the yield surface hardens isotropically up to a failure surface. In this range, the plastic strain rate is governed by the yield function. This criterion has the potential to consider cracking and crushing in concrete. Cracking potential from this model was used; however, Drucker-Prager yield criterion was employed instead of crushing potential of William-Warnke model to take the confinement effect into account.

Failure model that was considered for FRP was Tsai-Wu criterion (Tsai and Wu, 1971). This criterion is extensively used for anisotropic composite materials which have different strengths in tension and compression. Fam and Rizkalla (2001) showed that failure of the FRP tubes under combined axial compressive and hoop tensile stresses can be

successfully identified by the Tsai-Wu failure criterion. In this failure model, failure criterion is obtained by interacting and combining the allowable stresses in all directions.

Element Type and Modeling

Twelve cantilever RC columns were modeled using ANSYS; the general-purpose FE software. SOLID65, an eight-node brick element with three translation degrees of freedom per node, was used to model concrete volume. This element is capable of cracking in tension and crushing in compression, so that the post-cracking effect of concrete is included for assembling the total stiffness matrix (Musmar, 2013). SHELL99 is defined by eight nodes, average or corner layer thicknesses, layer material direction angles and orthotropic material properties. This element is well-suited for modeling layered FRP composite materials and was used to model FRP wrap. Considering that FRP sheets only resist tensile stresses, "tension-only" option of SHELL99 was activated. SOLID45 element was used for the steel plates at the support and the loading areas as rigid bodies to avoid divergence of nonlinear analyses due to the concentrated load effect on concrete. The FRP composite was considered as an orthotropic linear material with different elastic moduli in different directions. To limit the effect of the FRP jacket to confinement, its elastic modulus in all directions except the fiber direction was set close to zero. Both longitudinal and transverse reinforcements were modeled using 3D-element called Link8. This element has two nodes and three degrees of freedom for each node. The bond between concrete and reinforcements was assumed to be perfect. Concrete cohesion (C) and angle of internal friction (φ) properties were obtained from the Drucker-Prager criterion using Eqs. 13 and 14. The FE mesh of a column without FRP jacket is shown in Fig. 5.

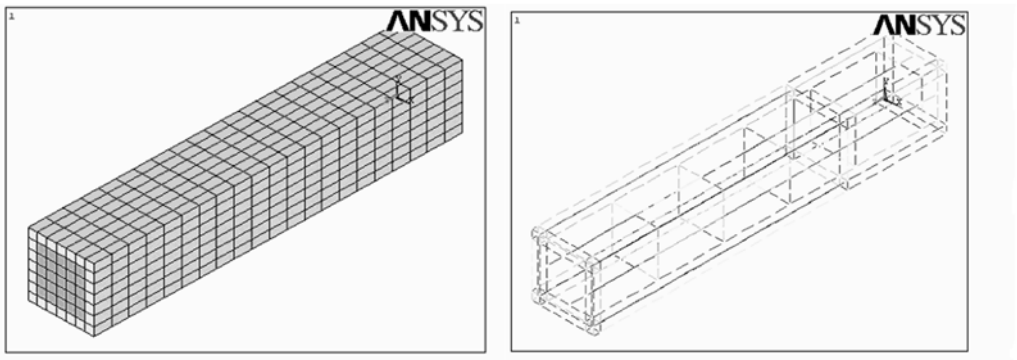

Figure (5): FE mesh of a column without FRP jacket

In order to examine the inelastic behavior of the column models, displacement-controlled pushover analysis was performed. Target displacement was set to 5 cm to conform to the experimental study. Axial load was kept constant during the analysis. In Fig. 6, the test setup for the experimental study is shown. Great attention was paid to mimic exactly the experimental conditions in the FE modeling. The bottom of the columns was restrained from displacement in x, y and z directions to simulate the boundary condition in the experiment, in which the columns were fixed in the foundation block that was bolted to a strong floor.

Figure (6): Test setup in the experimental study

RESULTS AND DISCUSSION

The key outcome of a pushover analysis is the lateral force-displacement relationship. The lateral force as a function of the top displacement for unretrofitted and retrofitted columns designed in accordance with ACI (Pre-1971) is shown in Fig. 7 and Fig. 8, respectively. As it was expected, the FRP wraps enhanced the performance of the columns. At the beginning of the analyses, the initial stiffnesses are all the same, since the axial load is the dominant force. However, their behavior is different in higher displacements (above 10 mm). It is clear from the plots that lateral load-carrying capacity of the columns was decreased by increasing the axial load. Retrofitted columns maintain the bearing load at high levels and their softening starts at higher displacements compared to their unretrofitted counterparts. These observations are consistent with experimental results.

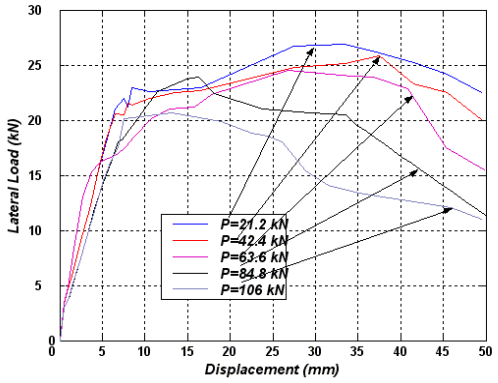

Figure (7): Capacity curves for unretrofitted columns designed according to ACI (Pre-1971)

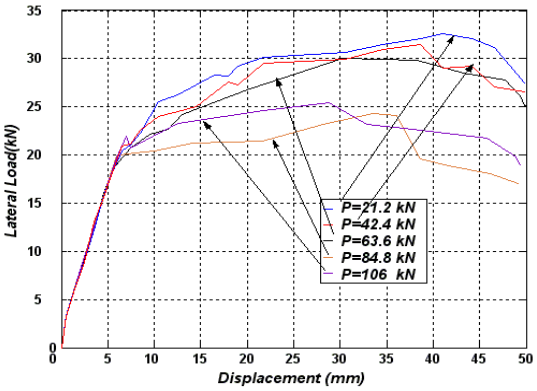

Figure (8): Capacity curves for retrofitted columns designed according to ACI (Pre-1971)

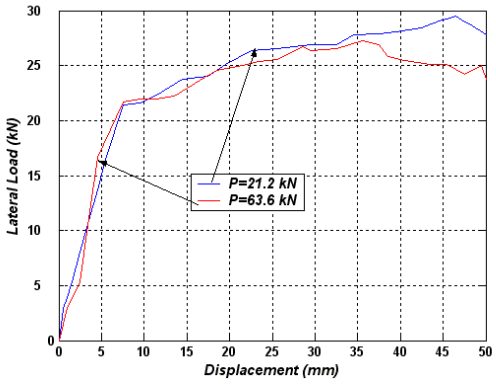

Figure (9): Capacity curves for columns designed according to ACI (318-02)

Fig. 9 exhibits capacity curves for the columns designed in accordance with ACI (318-02). Lateral load capacity of these columns was higher than that of the columns designed according to ACI (Pre-1971) in terms of both capacity and degradation. Comparison of lateral load-carrying capacity of the columns is summarized in Fig. 10. As indicated in the graph, the strengthening method could increase the capacity of the columns up to

22%, 22%, 22%, 10% and 17% for axial loads of 21.2, 42.4, 63.6, 84.8 and 106 kN, respectively.

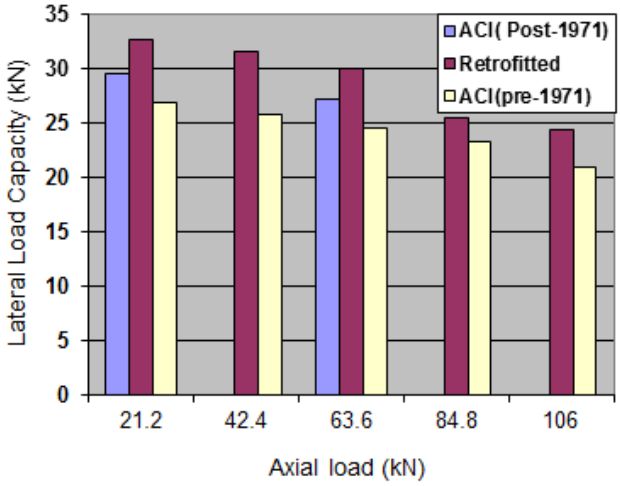

Figure (10): Lateral load-carrying capacities of the analyzed columns

In Fig. 11 to Fig.13, deformation of a retrofitted column, stress ratio on concrete in a retrofitted column and stress on FRP sheets based on the Tsai-Wu criterion with their corresponding experimental observations are displayed, respectively. As shown in Fig. 11, deformation of the column has started from the level after the strengthened zone, due to confined plastic hinge which led to higher stiffness. This means that FRP wrap can successfully move plastic hinge from the bottom of the column, which possesses poor confinement and highest shear and moment. In Fig. 12, stress concentration on concrete just above the FRP jacket is evident. Also, due to high tensile strength of fibers, all the stresses on the FRP sheets were in the elastic range as demonstrated in Fig.13. All these results are consistent with experimental observations as demonstrated in Fig. 11 to Fig. 13.

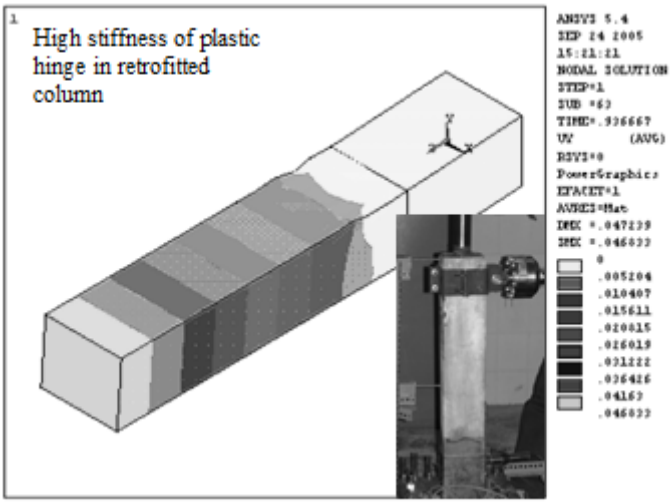

Figure (11): Contours of deformation on SP-C6 at 46.8 mm lateral displacement

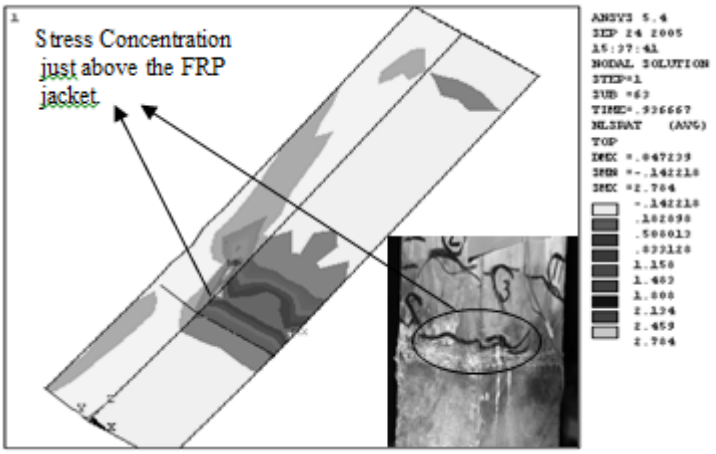

Figure (12): Contours of stress on SP-C8 at 46.8 mm lateral displacement

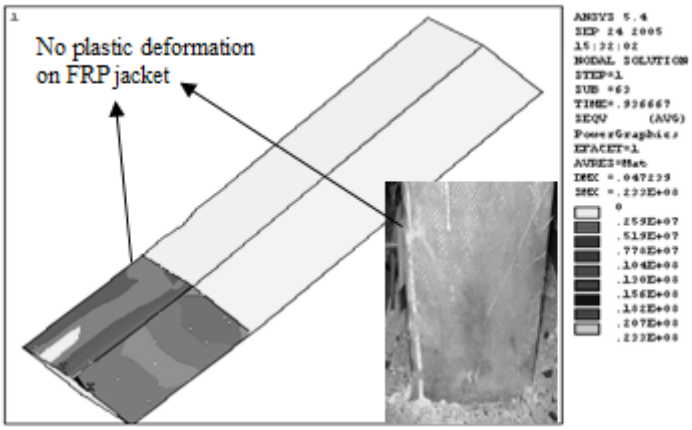

Figure (13): Contours of stress on SP-C7 based on Tsai-Wu criterion at 46.8 mm lateral displacement

Validation of the FE Model

An experimental study was conducted by the authors to validate the proposed FEA. Since in the experimental study the columns were tested under cyclic loading, the hysteresis loop envelope was compared with monotonic curves obtained from pushover analysis in FE modeling. Hysteresis loop envelope encloses the forces and displacements under cyclic loading and in many studies it has been compared with monotonic capacity curves, e.g. (Deierlein et al., 2010). Hysteresis loop envelope obtained from the experiment and capacity curve from pushover analysis for SP-C8 are exhibited in Fig. 14. The hysteresis loop envelope demonstrates sharp softening after 40 mm displacement, which can be due to cyclic loading that occurs as a result of concrete cracking, bond slip, Bauschinger effect,… etc. Numerical and experimental lateral load capacities for six specimens are summarized in Fig. 15. As indicated, the maximum error between experimental and numerical values is around 14% in SP-C8 and the minimum error is around 4% in SP-C1. The comparison between the experimental and the proposed FEA results shows reasonably good agreement. As such, the proposed FE models in the present study may be utilized as a tool to generate a very large database taking into account all the possible ranges of critical parameters affecting the behavior of a confined RC column.

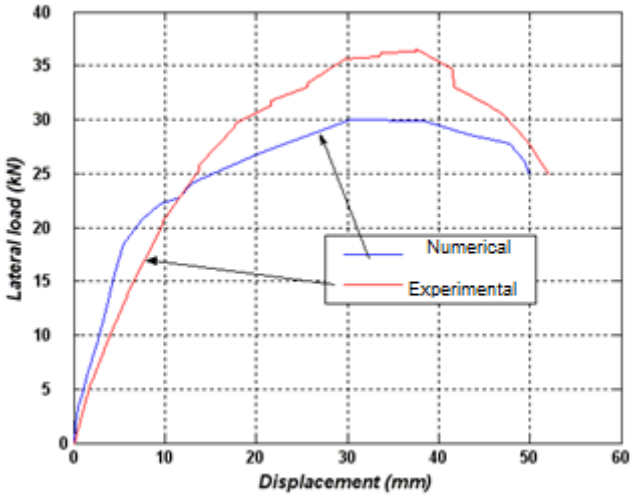

Figure (14): Numerical and experimental lateral load-carrying capacities *versus* displacement for SP-C8

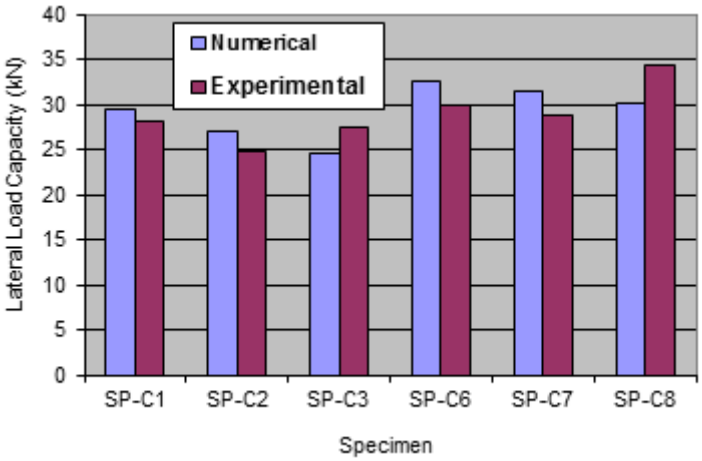

Figure (15): Numerical and experimental lateral load capacities of SP-C1, SP-C2, SP-C3, SP-C6, SP-C7 and SP-C8

CONCLUSIONS

Proper confinement in plastic hinge zone of RC columns has significant influence on the behavior of RC structures subjected to earthquake loading. However, many RC columns that were designed and constructed based on ACI (Pre-1971) have a poorly confined plastic hinge zone. The method of retrofitting plastic hinge zone of columns by GFRP can significantly enhance the performance of these columns. By increasing confinement, this method can increase shear capacity, ductility and bending strength. In this paper, an attempt was made to introduce a rational and comprehensive procedure for nonlinear FEA of FRP-strengthened slender RC columns with structural deficiency. Appropriate elements and constitutive material modeling from the software were chosen to account for the realistic behavior of the columns. Moreover, modeling and analysis procedures were verified using experimental results. The columns were investigated in

the conditions with and without FRP wrap and under different axial load levels. The conclusions drawn from this study can be summarized as follows:

1- The developed FE models were capable of predicting the lateral load–deflection behavior of both RC columns and FRP-strengthened RC columns. The failure modes predicted were the same as those experimentally observed.
2- FEA performed in this study clearly demonstrated that the externally bonded GFRP sheet is a practical solution towards enhancing shear and flexural strengths, as well as ductility of slender RC columns whose plastic hinge zones are reinforced with insufficient stirrups.
3- By increasing the axial load, load-carrying capacity of the columns was decreased. The reduction for unretrofitted columns was almost two times greater than for retrofitted ones.
4- By increasing axial load, stress and strain in FRP sheets were increased. There was a stress concentration on the sheets at the column corners, but no failure or plastic deformation was detected, which is consistent with experimental observations.
5- The wrapping GFRP sheet around the plastic hinge zone of the defective RC column provides not only enough shear strength, which results in a ductile flexural failure mode with the concept of strong shear and weak flexure. On the other hand, the confinement of concrete in the plastic hinge leads to an increase in the ductility of the RC column. With the confinement of GFRP, a desirable ductile flexural failure mode rather than a brittle shear failure mode can be achieved.
6- Similar to the experimental study, FEA revealed that wrapping only the plastic hinge can move the plastic hinge away from the bottom of the column. This is a critical consequence of this retrofitting technique for columns in the first floor of the building, as it does not lead to inhibiting the formation of plastic hinge, which is necessary for the mechanism in buildings during an earthquake.

REFERENCES

ACI Committee 440R-96 Report. (1996). "State-of-the-art report on fiber-reinforced plastic reinforcement for concrete structures". American Concrete Institute.

Ahmad, S.H., Khaloo, A.R., and Irshaid, A. (1991). "Behavior of concrete spirally confined by fiber glass filaments". Magazine of Concrete Research, 43 (156), 143-148.

Al-Dwaik, M.M., and Armouti, N.S. (2013). Analytical case study of seismic performance of retrofit strategies for reinforced concrete frames: steel bracing with shear links *versus* column Jacketing. Jordan Journal of Civil Engineering, 7 (1).

ANSYS. (2005). "ANSYS version 10 manual set 2005". ANSYS Inc., Southpointe, 275 Technology Drive, Canonsburg, PA 15317, USA.

Bsisu, K. A. D., Hunaiti, Y., and Younes, R. (2012). "Flexural ductility behavior of strengthened reinforced concrete beams using steel and CFRP plates". Jordan Journal of Civil Engineering, 6 (3).

Campione, G., Miraglia, N., and Scibilia, N. (2001). "Compressive behavior of R.C. members strengthened with carbon fiber-reinforced plastic layers". International Conference on Earthquake Resistant Engineering Structures III, Malaga, Spain, 397-406.

Chaallal, O., Hassan, M., and Shahawy, M. (2003). "Confinement model for axially loaded short rectangular columns strengthened with fiber-reinforced polymer wrapping". ACI Structural Journal, 100 (2), 215-221.

Chen, B., and Mau, S.T. (1989). "Recalibration of a plastic-fracturing model for concrete confinement". Cement and Concrete Research, 19 (1), 143-154.

Chen, W.-F. (1982). "Plasticity in reinforced concrete". New York: McGraw-Hill Company, 816 p.

Chung, H. S., Yang, K. H., Lee, Y. H., and Eun, H. C. (2002). "Stress-strain curve of laterally confined concrete". Cement and Concrete Composites, 24 (9), 1153-1163.

Deierlein, G., Reinhorn, A.M., and Willford, M. (2010). "Nonlinear structural analysis for seismic design". NEHRP Seismic Design Technical Brief, No. 4 (NIST GCR 10-917-5).

Einde, L.V.D., Zhao, L., and Seible, F. (2003). "Use of FRP composites in civil structural applications". Construction and Building Materials, 17 (6-7), 389-403.

Eshghi, S., and Zanjanizadeh, V. (2007). "Repair of earthquake-damaged square R/C columns with glass fiber-reinforced polymer." International Journal of Civil Engineering, 5 (3), 210-223.

Eshghi, S., and Zanjanizadeh, V. (2008). "Cyclic behavior of slender R.C. columns with insufficient lap splice length". 14th World Conference on Earthquake Engineering (14WCEE), Beijing, China, Paper ID: 12-03-0004.

Eshghi, S., and Zanjanizadeh, V. (2008). "Finite element modeling of retrofitted reinforced concrete columns with glass fiber-reinforced polymer." Scientific Research Journal of Sharif University of Technology, 40, 21-28.

Eshghi, S., and Zanjanizadeh, V. (2008). "Retrofit of slender square concrete columns by glass fiber-reinforced polymer for seismic resistance." Iranian Science and Technology Journal, 32 (B5), 437-450.

Fam, A., and Rizkalla, S. (2001). "Confinement model for axially loaded concrete confined by circular fiber-reinforced tubes". ACI Structural Journal, 98 (4), 451-461.

Fardis, M.N., and Khalili, H. (1981). "Concrete encased in fiber glass-reinforced plastic". ACI Journal, (78), 440-446.

Issa, M.A., and Alrousan, R.Z. (2009). "Experimental and parametric study of circular short columns confined with CFRP composites". Journal of Composites for Construction, 13 (2), 135-147.

Jiang, T., and Teng, J. (2013). "Behavior and design of slender FRP-confined circular RC columns". Journal of Composites for Construction, 17 (4), 443-453.

Karabinis, A., and Rousakis, T.C. (2002). "Concrete confined by FRP material: a plasticity approach". Engineering Structures, 24 (7), 923-932.

Kawashima, K., Hosotani, M., and Yoneda, K. (2001). "Carbon fiber sheet retrofit of reinforced concrete bridge bents". Toward New Generation Seismic Design Methodology of Bridges, Institute of Technology, Tokyo, Japan.

Pulido, C., Saiidi, S. M., Sanders, D., Itani, A., and El-Azaay, S. (2004). "Seismic performance of two-column bents-part1: retrofit with carbon fiber-reinforced polymer fabrics". ACI Structural Journal, 101 (4), 558-568.

Kent, D.C., and Park, R. (1971). "Flexural members with confined concrete". Journal of Structural Division, 97 (ST7), 1969-1990.

Loud, S. (1995). "California prepares for 'the big one' with composite retrofitting technology".

Lynn, A. C., Moehle, J. P., Mahin, S. A., and Holmes, W.T. (1996). "Seismic evaluation of existing reinforced concrete building column". Earthquake Spectra, 12 (4), 715-739.

Mander, J. B., Priestley, M. J. N., and Park, R. (1988). "Theoretical stress–strain model for confined concrete". Journal of Structural Engineering, 114 (8), 1804-1826.

Masukawa, J., Akiyama, H., and Saito, H. (1997). "Retrofitting of existing reinforced concrete piers by using carbon fiber sheet and aramid fiber sheet". Proceedings of the Third International Symposium on Non-metallic (FRP) Reinforcement for Concrete Structures, 411-418.

Melek, M., and Wallace, J.W. (2004). "Cyclic behavior of columns with short lap splices". ACI Structural Journal, 101 (6), 802-811.

Mirmiran, A., Zagers, K., and Yuan, W. (2000). "Nonlinear finite element modeling of concrete confined by fiber composites". Finite Element in Analysis and Design, 35 (1), 79-96.

Moehle, J.P., Ghannoum, W., and Bozorgnia, Y. (2006). "Collapse of lightly confined reinforced concrete frames during earthquakes". In: Wasti, S.T. and Ozcebe, G. (Eds.), Advances in Earthquake Engineering for Urban Risk Reduction, Nato Science Series-IV: Earth and Environmental Sciences. Springer, Netherlands, 317-332.

Musmar, M.A. (2013). "Analysis of shear wall with openings using solid65 element. Jordan Journal of Civil Engineering, 7 (2).

Nanni, A., and Bradford, N.M. (1995). "FRP-jacketed concrete under uniaxial compression". Construction and Building Materials, 9 (2), 115-124.

Obaidat, Y.T. (2013). "Effect of interfacial properties on the behaviour of retrofitted members". Jordan Journal of Civil Engineering, 7 (2).

Park, R., Priestley, M. J., and Gill, W. D. (1982). "Ductility of square-confined concrete columns". Journal of Structural Engineering, 108 (ST4), 135-137.

Parvin, A., and Wang, W. (2001). "Behavior of FRP-jacketed concrete columns under eccentric loading". Journal of Composites for Construction, 5 (3), 146-152.

Feng, P., Lu, X. Z., and Ye, L. P. (2002). "Experimental research and finite element analysis of square concrete columns confined by FRP sheets under uniaxial compression". Proceedings of 17th Australasian Conference on the Mechanics of Structures and Materials, Gold Coast, Australia, 71-76.

Pellegrino, C., and Modena, C. (2010). "Analytical model for FRP confinement of concrete columns with and without internal steel reinforcement". Journal of Composites for Construction, 14 (6), 693-705.

Penelis, G., and Kappos, A.J. (1997). "Earthquake-resistant concrete structures." E and FN Spon Published.

Priestley, M., Sieble, F., Xiao, Y., and Verma, R. (1994). "Steel jacket retrofitting of reinforced concrete bridge columns for enhanced shear strength – part II: test results and comparison with theory". ACI Structural Journal, (91), 537-551.

Rochette, P., and Labossiere, P. (1996) "A plasticity approach for concrete columns confined with composite materials". Proceedings of Advanced Composite Materials in Bridges and Structures, CSCE, 359-366.

Samaan, M., Mirmiran, A., and Shahawy, M. (1998). "Model of concrete confined by fiber composites". Journal of Structural Engineering, 124 (9), 1025-1031.

Sheikh, S.A., and Li, Y. (2007). "Design of FRP confinement for square concrete columns". Engineering Structure, 29 (6), 1074-1083.

Silva, M.A.G. (2011). "Behavior of square and circular columns strengthened with aramidic or carbon fibers". Construction and Building Materials, 25 (8), 3222-3228.

Tamuzs, V., Tepfers, R., Zile, E., and Valdmanis, V. (2007). "Stability of round concrete columns confined by composite wrappings". Mechanics of Composite Materials, 43 (5), 445-452.

Teng, J.G., Chen, J.F., Smith, S.T., and Lam, L. (2002). "FRP-strengthened RC structures". John Wiley and Sons, UK.

Tsai, S. W., and Wu, E. M. (1971). "A general theory of strength for anisotropic materials". Journal of Composite Materials, 5 (1), 58-80.

Willam, K. J., and Warnke, E. P. (1975). "Constitutive models for the triaxial behavior of concrete". Proceedings of the International Assoc. for Bridge and Structural Engineering, 19, 1- 30.

Wu, G., Wu, Z.S., and Lu, Z.T. (2007). "Design-oriented stress–strain model for concrete prisms confined with FRP composites". Construction and Building Materials, 21 (5), 1107-1121.

Xiao, Y., Wu, H., and Martin, G. (1999). "Pre-fabricated composite jacketing of RC columns for enhanced shear strength". ACI Structural Journal, (125), 255-264.

Yu, T., Teng, J.G., Wong, Y.L., and Dong, S.L. (2010). "Finite element modeling of confined concrete-I: Drucker–Prager type plasticity model". Engineering Structures, 32 (3), 665-679.